

Triethylene Glycol Dehydration of Natural Gas: Evaluation of Mass and Heat Transfer Coefficients in the Case of Absorption and Stripping Structured Packing Towers



This work is licensed under a Creative Commons Attribution 4.0 International License

A.-D. Filep, T. Todinca,* and G.-A. Dumitrel

University Politehnica of Timișoara, Faculty of Industrial Chemistry and Environmental Engineering, 6 Vasile Pârvan Boulevard, 300223 Timișoara, România

doi: <https://doi.org/10.15255/CABEQ.2021.1998>

Original scientific paper

Received: July 24, 2021

Accepted: December 13, 2021

In the last decades, due to their hydraulic performances, structured packings have become the main internals in TEG dehydration units. However, the available literature correlations for the evaluation of mass and heat transfer coefficients were found inaccurate for this process. In this work, the values of mass transfer coefficients were estimated by minimizing the differences between models predictions and industrial plants data. Results show that, for absorber, the gas overall mass transfer coefficient, K_{yg} , strongly depends on the F factor, while liquid load effect remains relatively low. For the stripper, the volumetric mass transfer coefficient, K_{ya} , was expressed as a function of the F factor and of the liquid load. On absorber heat transfer side, the Nusselt number correlation parameters were estimated using heat transfer coefficient values based on heat balance. The heat flux was found 2.5 times higher than the predictions based on Chilton – Colburn analogy.

Keywords:

TEG dehydration, HYSYS flowsheeting, mass and heat transfer coefficients, stripping column, TEG contactor

Introduction

In hydrocarbons extraction through wellheads, the fluid (oil, gas, and water) is processed in order to meet the requirements for hydrocarbons transportation and valorization and for water release into the environment.

The gas phase, usually known as “natural gas”, in which the major component is methane, and in lower amounts, other light hydrocarbons, also contains components that are dangerous from the standpoint of both pipeline transportation and further gas processing. One of these components is water, because of its possibility to create corrosion (in liquid phase, if acid gases are present) and to form ice or gas hydrates depending on the operating conditions¹.

The allowable amount of water in natural gas distribution systems is specified by the dew point temperature at a specific pressure (like in Europe) or by the content of water per unit of volume of gas (pounds per million standard cubic feet, US and Canada). In Romania, the maximum water dew point temperature is usually $-15\text{ }^{\circ}\text{C}$ in the entire range of operating pressure of the transportation system. It also has to be mentioned that further re-

moval may be required upstream of a gas liquefaction unit or of other gas processing units.

Among the well-known methods for drying natural gas (compression and cooling, absorption in selective liquids, adsorption on solid desiccants, hydration of deliquescent compounds, etc.), one of the most widely used is counter-current absorption using glycols. Although several glycols (ethylene glycol, diethylene glycol, triethylene glycol, tetraethylene glycol) can be used for industrial applications in natural gas drying, triethylene glycol (TEG) is the preferred glycol because of its high absorption capacity and thermal stability. Also, due to small vapor pressure, losses caused by evaporation are very small².

In its simplest configuration, a TEG dehydration unit (Fig. 1) contains a contactor (counter-current absorber), a flash tank which acts as a phase separator (the pressure of the rich TEG is decreased for values around 4–5 bar for the separation of absorbed hydrocarbons), rich/lean TEG heat exchanger (lean TEG going to contactor is cooled down by the rich TEG), filters, and a regeneration unit where water is removed from the TEG. This unit could consist merely of a column where the rich TEG enters between its heat transfer (bottom) and rectification (top) sections, and a reboiler where the necessary heat for water boiling out of the TEG is provided by firing natural gas or electrically.

*Corresponding author: tel: +40256403169, Fax: +40256403060; E-mail: teodor.todinca@upt.ro

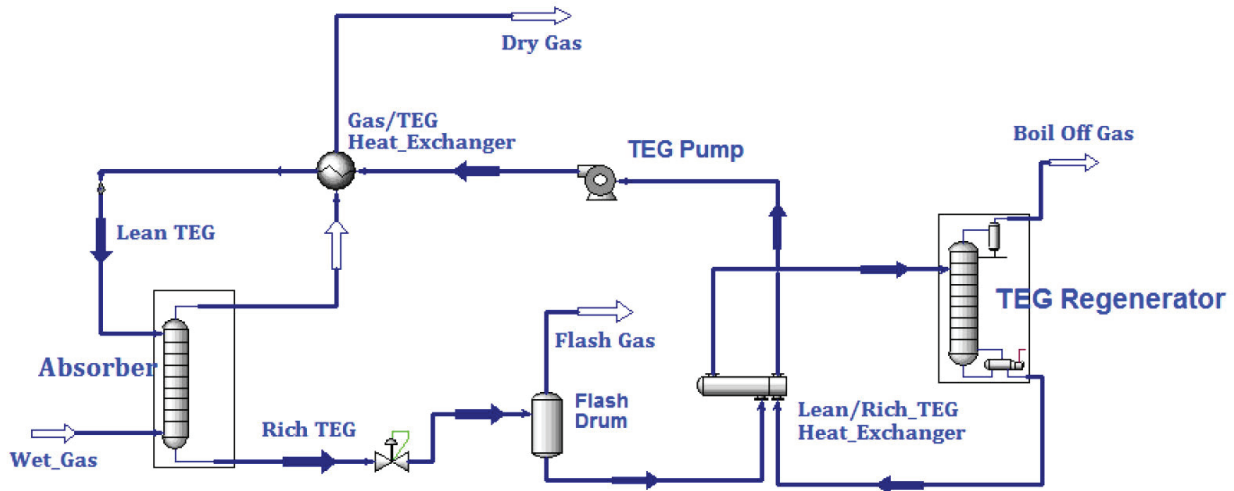


Fig. 1 – Typical TEG dehydration unit

Such configuration is unable to reach a high regeneration degree because the temperature in the reboiler is limited to a maximum of 204 °C (TEG decomposition sharply increases at higher temperatures) and at an operating pressure close to atmospheric pressure, the TEG in lean (strong) solution can reach around 98.8 w%. In case this is not enough to satisfy natural gas water content specification, one way to increase the TEG regeneration up to 99.9 w% is by using a stripping gas that is injected in the bottom of the regenerator or in the reboiler. Other methods to enhance the stripping of glycol to higher purities are described in the literature^{3–5}:

- The “Drizo” process, used for stripping a recoverable agent (examples: n-heptane, iso-octane or aromatic hydrocarbons), which is recovered in its liquid state by cooling (after the still column) and recycled to regeneration;

- The stripping gas and the Stahl column (stripping column), located beyond the reboiler (the stripping gas, injected into the bottom of the Stahl column circulates in counter current with the lean TEG from the reboiler, while the overhead of the column is directed to the bottom of the regeneration column or to the reboiler);

- The “Coldfinger” utilizes a cooling coil in the vapor space of a surge tank to increase the glycol regeneration further.

In many natural gas TEG dehydration units, the stripping column is placed between a surge tank and the reboiler (Fig. 2).

In the last decades, due to their hydraulic performances, structured packings, such as Sulzer Mellapak M250Y, have become the first option for internals in the contactor and stripping columns of TEG dehydration units. In still columns, other packings, like I-rings, are encountered in some configurations.

The total height of the columns can be calculated by multiplying the number of theoretical stages (NTS) with the height equivalent to a theoretical plate (HETP). In TEG dehydration, the HETP values are more of a rule of thumb recommendation than an accurate evaluation that depends on the operating parameters. At the same time, despite the numerous works dedicated to the mass transfer correlations for structured packings^{6–10}, when compared to TEG dehydration units real data, none of these were found accurate enough to correctly predict packing performance. Therefore, in this paper, the values of the mass and heat transfer coefficients were estimated using data from three industrial units manufactured by Armax Gaz SA (Medias, Romania). Because not all process operating data for such estimation could be measured directly, the Aspen HYSYS[®] simulation package¹¹ was used for data validation and reconciliation.

HYSYS simulation of natural gas dehydration with TEG

Since the 1970s, when the first interactive process simulator (HYSIM of HYPROTECH Ltd.) became available for process flowsheeting, the ability of process simulators to accurately design and rate industrial units increased strongly in both components/mixtures properties prediction and equipment/plants modeling and simulation. In TEG dehydration of natural gas, some of the widely used simulation packages are Aspen HYSYS (Aspen Tech), UNISIM (Honeywell), Aspen Plus (Aspen Tech), Pro II (SimSci), CHEMCAD (Chemstations), ProSimPlus (ProSim), ProMax (Bryan Research Engineering), etc. Because of its special/dedicated property packages, and the possibility to integrate new equipment models (through Aspen Custom Model-

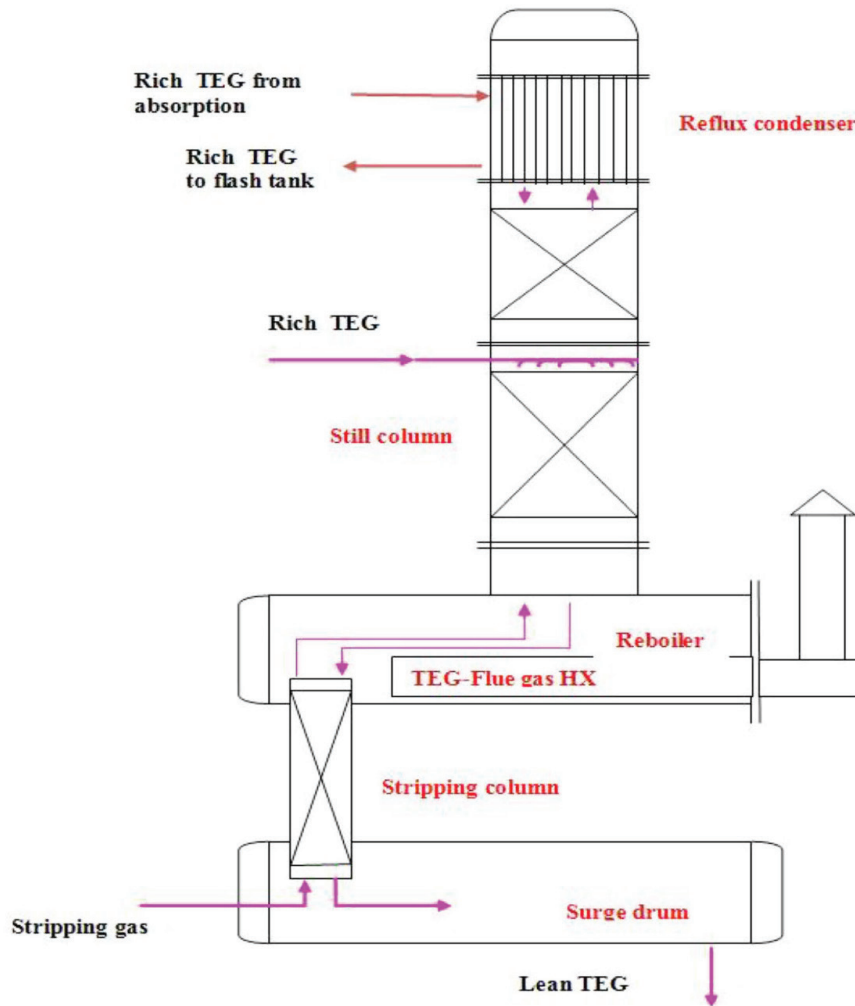


Fig. 2 – Regeneration: Increased TEG purity using the stripping gas

er) or to interconnect the process flowsheet with other Aspen Tech software components, Aspen HYSYS® was used in this work.

Aspen HYSYS includes a specially designed properties evaluation tool, the Glycol package, which is based on Twu-Sim-Tassone EOS. TST was improved¹² in order to be able to predict activity coefficients and water content in the operating range encountered in TEG dehydration units. Our accuracy checks regarding the hydrocarbons solubility in TEG, the evaluation of water dew point and water/TEG equilibrium using experimental data^{12–16}, confirmed the Glycol package (incorporated in Aspen HYSYS 8.6) as a good option for building up simulation cases for the validation and reconciliation of the process data for the purpose of evaluating the mass and heat transfer coefficients. More recently (2018), by incorporation of Cubic Plus Association (CPA) package in HYSYS (starting with version 10), Aspen Tech also recommends this package for the modeling of dehydration units¹³.

The simulation scheme used in this work is presented in Fig. 3. Usually, the dehydration zone

of the unit consists of an inlet separator, contactor (C-001), and gas/TEG heat exchanger (HX-001). The inlet separator, built as detached equipment or in the bottom zone of the absorption tower, has the role of retaining any condensed liquid from the gas before entering the contactor. In order to evaluate the water dew point of the dried gas, a component splitter (X-1) is used for extracting the TEG vapor from the flux that leaves the gas/TEG heat exchanger (HX-001). The splitter, which is not a physical unit, is included in the scheme for avoiding a TEG vapor negative effect on the accuracy of the dew point calculation. A balance operation (BAL-1) can be inserted for the evaluation of the water dew point at another pressure than the actual pressure.

The rich TEG leaving the contactor is sent through the valve V-001 and the reflux condenser RC-003 (simulated by a heat exchanger, HX-003, and a separator, S-003) to the S-002 separator. Normally, because of the presence of heavy hydrocarbons and TEG degradation compounds, etc., in the liquid phase, a three-phase separator is used in TEG dehydration plants. In the units where the pressure

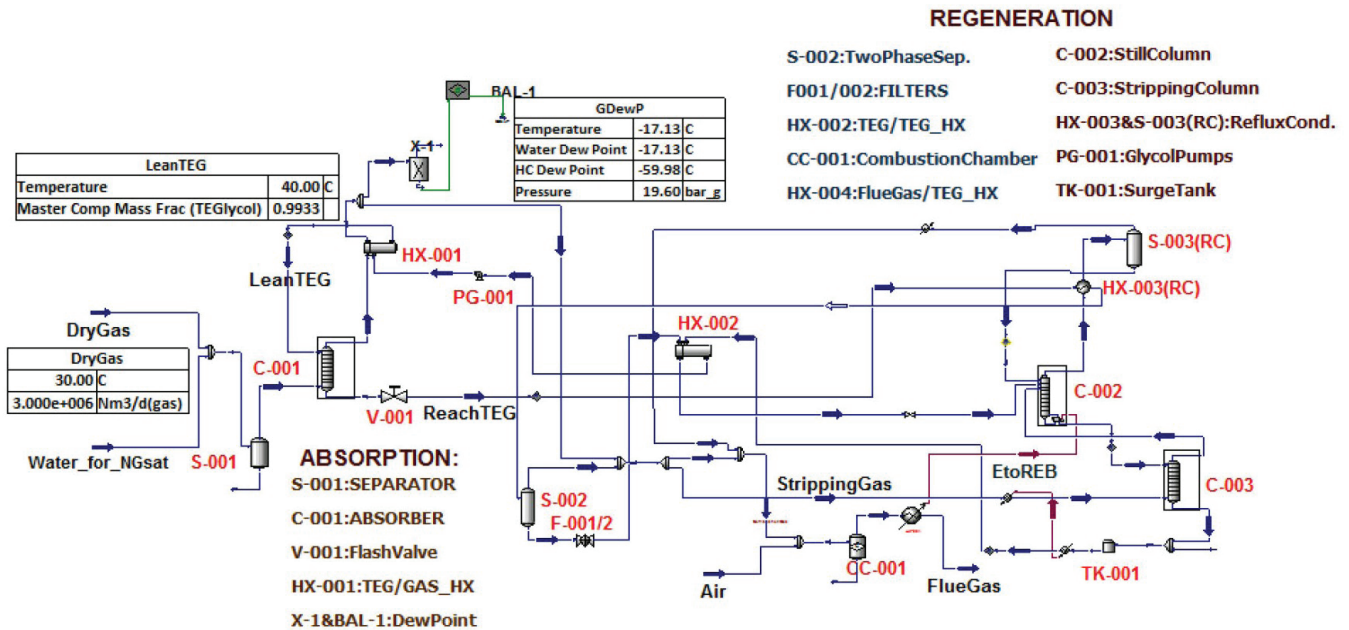


Fig. 3 – Simulation scheme of a typical natural gas TEG dehydration unit

in the contactor is very high, flashing of the rich TEG for hydrocarbons removal takes place before it works as a cooling agent in the top of the still column. To generate both stripping and combustion streams, a combination of flash gas from the S-002 separator with a flux diverted from dried gas is implemented.

The boil-off gas resulting from the still column is also valorized in the combustion chamber: this way, the stripping gas is entirely used to generate heat and water vapor, which are used as heat carriers in the flue-gas/TEG heat exchanger. In the CC-001 combustion chamber, combustion reactions of all hydrocarbons and TEG vapor are taken into account for heat generation. Few recycle units are implemented in order to facilitate the convergence of the simulation scheme or to analyze the different zones of the process independently.

Mass and heat transfer coefficients evaluation: Experimental data, modeling, and tuning of the model parameters

Wet gas – TEG contactor

In a previous work¹⁷, mass and heat transfer occurring in the absorption column of the TEG dehydration process have been evaluated on a volumetric basis. The plant data from three different units covered liquid loads ranging from 1.2 to 2.5 m³ m⁻² h⁻¹, pressures between 16 to 41 bar, *F* factors ranging from 0.7 to 2.5 Pa^{0.5} and average gas inlet temperatures ranging from 15 to 42 °C. In the present work, in order to increase the accuracy of composition

and temperature profiles, the data were reevaluated for the purpose of accounting for the gas – liquid contact area and the direct contact gas-liquid heat transfer coefficient.

Data regarding wetted area for M250Y structured packing are presented by Tsai¹⁸, the ratio of the effective to specific area being expressed by the relation:

$$\frac{a}{a_p} = 1.34 \cdot \left[\frac{\rho_L}{\sigma} \cdot g^{0.33} \cdot \left(\frac{L_V}{L_p} \right)^{1.33} \right]^{0.116} \quad (1)$$

Equation 1 is based on the data ranging from 2 to 60 m³ m⁻² h⁻¹. Viewing the range of our liquid load data, a correction factor of 1.12 was inserted in equation (1) based on the Tsai experimental data inferior zone (up to 10 m³ m⁻² h⁻¹).

Evaluation of direct contact heat transfer coefficient

For the evaluation of the gas – liquid direct contact heat transfer coefficient, 11 sets of process data were checked for mass and heat balances using Aspen HYSYS (version 8.6). In order to account for the liquid distributor zone, a supplementary heat transfer area equivalent to 10 % of the gas liquid contact surface corresponding to the height equivalent to a theoretical plate (HETP) was taken into account and the liquid temperature at the top of the structured packing was reevaluated. In an approach similar to Spiegel and Bomio¹⁹, the value of the heat transfer coefficient, α_p , was calculated by analogy with the theory of multitubular heat exchangers: based on process simulation using Aspen HYSYS, heat flux Q_p and mean logarithmic difference tem-

Table 1 – Process and simulation data used for the evaluation of gas – liquid heat transfer coefficient

Parameter	Value	Parameter	Value
Packing nominal surface	250 m ² m ⁻³	Operating pressure	26.5 barg
Liquid inlet temperature	28 °C	Liquid temp., packing top	27.50 °C
Liquid outlet temperature	26 °C	Gas temp., packing top	26.80 °C
Gas inlet temperature	25 °C	Column diameter	2.1 m
Packing height	5.4 m	Gas superficial velocity	0.57 m s ⁻¹
Liquid load	1.2 m ³ m ⁻² h ⁻¹	Effective interfacial area	165 m ² m ⁻³
Heat flow transfer	480 kW (latent: 55 kW)	Heat transfer coefficient	185 W m ⁻² °C ⁻¹

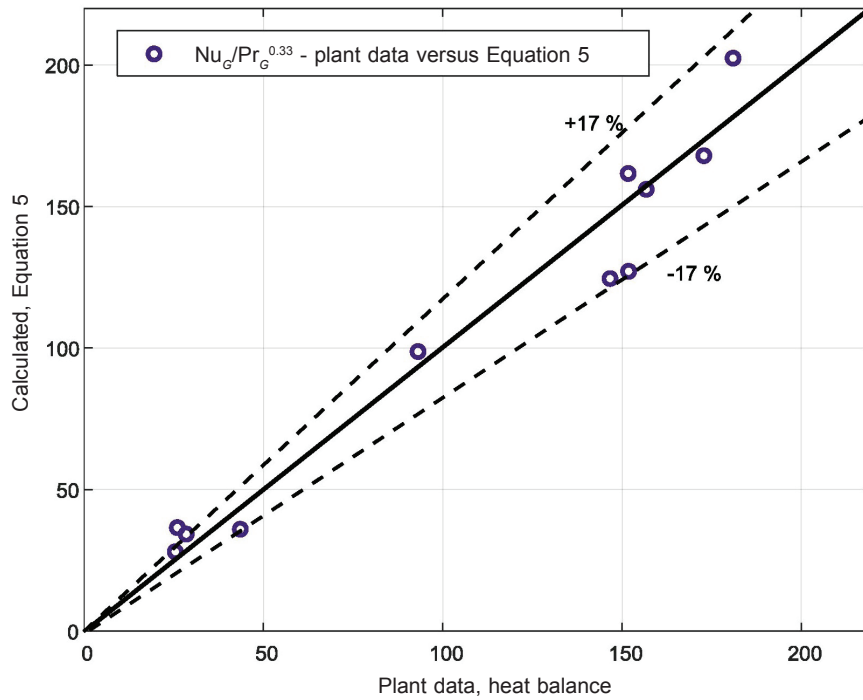


Fig. 4 – Nusselt number ($Nu_G/(Pr_G)^{0.33}$): Plant data estimations versus Equation 5

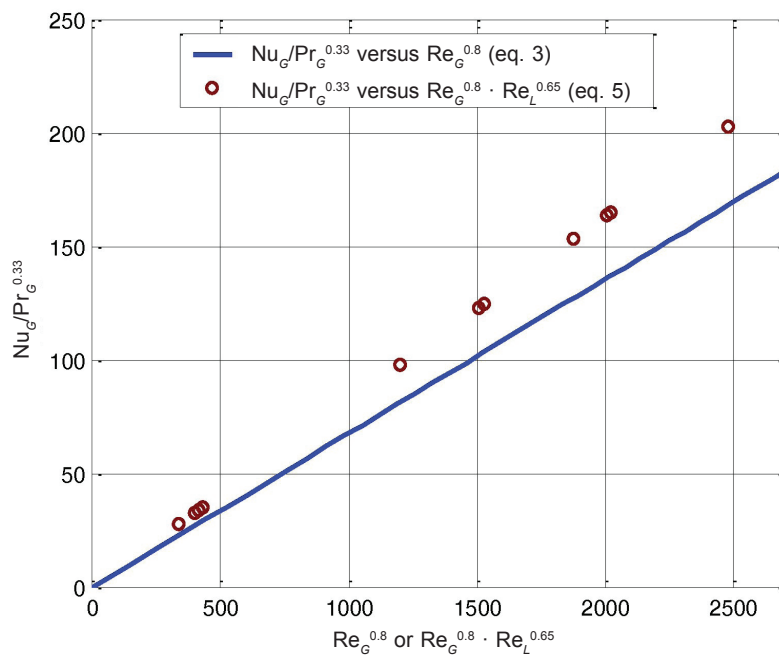


Fig. 5 – Values of the Nusselt number ($Nu_G/(Pr_G)^{0.33}$) as calculated by Equations 3 and 5

perature ΔT_{ML} were evaluated, followed by the calculation of the gas-liquid heat transfer coefficient (A – heat transfer area):

$$\alpha_T = \frac{Q_T}{A \cdot \Delta T_{ML}} \quad (2)$$

A typical set of data is presented in Table 1 (unit nominal capacity: $3 \cdot 10^6$ N m³ d⁻¹).

Spiegel and Bomio¹⁹ evaluation of the direct contact heat transfer coefficient based on sensible heat for different types of structured packings used in industrial applications lead to the following correlation:

$$Nu_G = 0.068 \cdot Re_G^{0.8} \cdot Pr_G^{1/3} \quad (3)$$

In the case of the natural gas-TEG contactor, after looking at the low values of liquid stripping densities and the small contribution of the latent heat to the total heat flux that has been transferred (with a maximum below 15 %), we also added the liquid Reynolds number on the right side of the Equation 3:

$$Nu_G = \phi_1 \cdot Re_G^{\phi_2} \cdot Re_L^{\phi_3} Pr_G^{1/3} \quad (4)$$

The parameters ϕ_1 , ϕ_2 and ϕ_3 have been evaluated by minimizing the square sum of the differences between the values of the heat transfer coefficient calculated based on the heat balance and the predictions of Equation 4. Because the first estimation of ϕ_2 was close to 0.8, we reviewed the values of the first and the last parameters in order to keep 0.8 as power for the gas Reynolds number. The result is:

$$Nu_G = 0.082 \cdot Re_G^{0.8} \cdot Re_L^{0.65} Pr_G^{1/3} \quad (5)$$

A comparison of $Nu_G / (Pr_G)^{0.33}$ predicted by Equation 5 and the values estimated on the basis of plant data is presented in Fig. 4. Considering the difficulties in the evaluation of temperature differences at the top and the bottom of the structured packing, the correlation accuracy can be considered acceptable.

The differences between Nu_G to Pr_G ratio predicted by Equations 3 and 5 from Fig. 5 could be

explained, at least partially, by the inclusion of latent heat in the evaluation of heat transfer in the last equation.

Evaluation of direct contact overall gas side mass transfer coefficient

The simplest estimation of the overall gas side mass transfer coefficient can be realized on the basis of operating and equilibrium lines in an x-y diagram¹⁷. Such an approach does not account for non-ideal phases behavior, temperature modification along tower axis, etc. Therefore, a non-isothermal plug flow model describing phase composition and temperature profiles along tower dimensionless axial coordinate was used. Due to low content of water in the gas phase, the gas molar flow rate was considered constant along tower axis, while the gas-liquid mass transfer of other components was neglected. The model also accounts for effective interfacial area (Equation 1) and direct contact overall gas phase heat transfer coefficient (Equation 5). A similar model was used by Saimpert *et al.*²⁰ for the modeling of absorption/desorption towers in the case of a CO₂ capture process using monoethanolamine. Model equations, developed in MATLAB®, are listed below:

- Molar liquid flow rate modification along tower axis is due only to water absorption:

$$\frac{dL}{dz} = -K_y \cdot a \cdot H \cdot S \cdot (y_w - y_w^*) \quad (6)$$

- In the water gas phase molar balance, the gas flow rate is considered constant:

$$\frac{dy_w}{dz} = -\frac{K_y \cdot a \cdot H \cdot S}{G} \cdot (y_w - y_w^*) \quad (7)$$

- The water molar balance in the liquid phase accounts for the liquid molar flow rate variation:

$$\frac{dx_w}{dz} = -\frac{K_y \cdot a \cdot H \cdot S}{L} \cdot (y_w - y_w^*) - \frac{x_w}{L} \cdot \frac{dL}{dz} \quad (8)$$

- The gas and liquid temperature modifications along the tower axis are due to direct contact heat transfer between phases and the heat flux associated with water transfer in the liquid phase. The heat of absorption only adds energy to the liquid phase:

$$\frac{dT_G}{dz} = \frac{\alpha_T \cdot a \cdot (T_L - T_G) \cdot H \cdot S - K_y \cdot a \cdot H \cdot S \cdot (y_w - y_w^*) \cdot c_M^G \cdot T_G}{G \cdot c_M^G} \quad (9)$$

$$\frac{dT_L}{dz} = \frac{-\alpha_T \cdot a \cdot (T_L - T_G) \cdot H \cdot S + K_y \cdot a \cdot H \cdot S \cdot (y_w - y_w^*) \cdot (\Delta H_{abs} + c_M^G \cdot T_G) - T_L \cdot c_{SL} \cdot \frac{dL_M}{dz}}{L_M \cdot c_{SL}} \quad (10)$$

Boundary conditions:

$$\begin{aligned} - \text{ at } z = 0 \quad y_w &= y_w^{btm} & T_G &= T_G^{btm} \\ - \text{ at } z = 1 \quad x_w &= x_w^{top} & T_L &= T_L^{top} & L &= L^{top} \end{aligned} \quad (11)$$

In the model, the methodology of Parrish *et al.*²¹ was used for the calculation of water and TEG activities:

$$\ln(\gamma_{\text{TEG}}) = \frac{B^2 \cdot \ln[\cosh(\tau)]}{A} - \frac{x_w \cdot B \cdot \tanh(\tau)}{x_{\text{TEG}}} - C^2 \cdot x_w^2 \tag{12}$$

$$\ln(\gamma_w) = B \cdot [\tanh(\tau) - 1] - C \cdot x_{\text{TEG}}^2 \tag{13}$$

where:

$$\tau = \frac{A \cdot x_w}{B \cdot x_{\text{TEG}}} \tag{14}$$

$$A = \exp(-12.792 + 0.03293 \cdot T_K) \tag{15}$$

$$B = \exp(0.77377 - 0.00695 \cdot T_K) \tag{16}$$

$$C = 0.88874 - 0.001915 \cdot T_K \tag{17}$$

The water equilibrium mole fraction accounts for the water activity in the liquid phase:

$$y_w^* = x_w \cdot \gamma_w \cdot \frac{P_w^{\text{sat}}}{P \cdot \phi_w} \tag{18}$$

Two parameters, K_y and α_T , initially calculated on the basis of the volumetric mass transfer coefficient¹⁷ and, respectively, on Equation 5, were tuned in order to reach plant data (as validated by Aspen HYSYS). Because reaching gas and liquid tempera-

ture at the top of the absorber while tuning K_y and α_T was inaccurate in some cases, the integration of Equations 6–10 started from the top of the contactor. Two examples are presented in Figs. 6 and 7.

Example 1. Main parameters: F factor $2.1 \text{ Pa}^{0.5}$, liquid load $1.47 \text{ m}^3 \text{ m}^{-2} \text{ h}^{-1}$

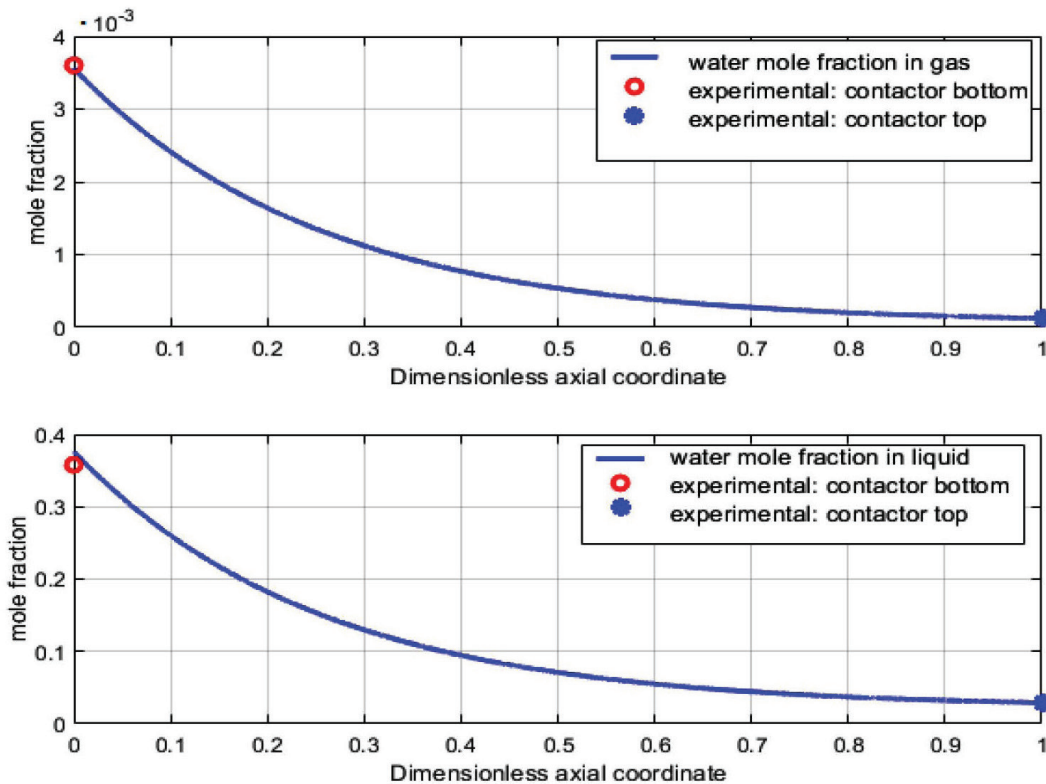


Fig. 6a – Example 1. Composition profiles (water mole fraction) of gas and liquid phases

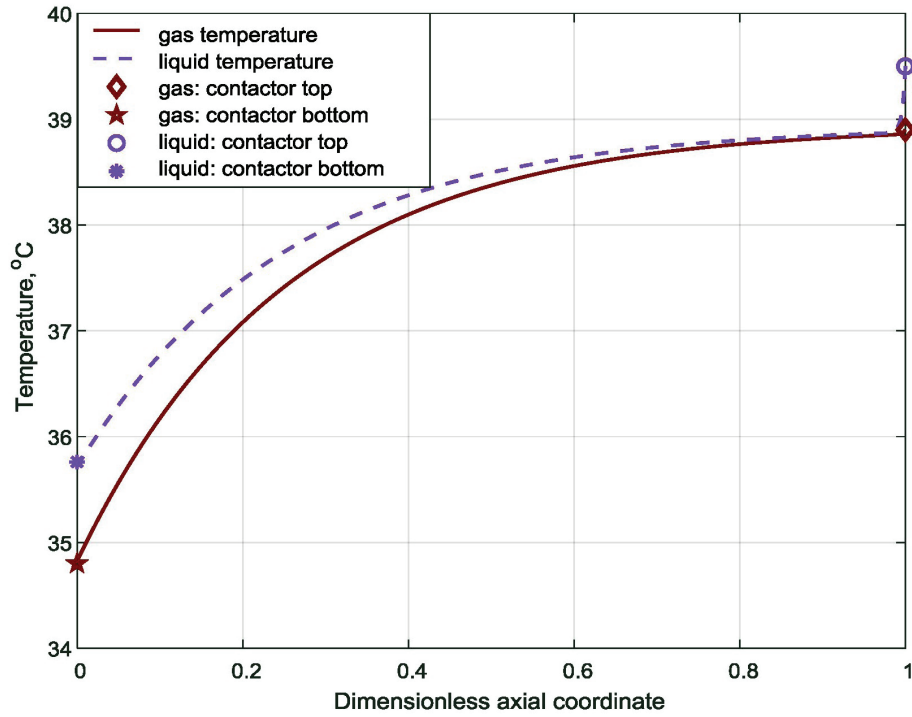


Fig. 6b – Example 1. Gas and liquid temperature profiles

Example 2. Main parameters: F factor $0.35 \text{ Pa}^{0.5}$, liquid load $1.3 \text{ m}^3 \text{ m}^{-2} \text{ h}^{-1}$

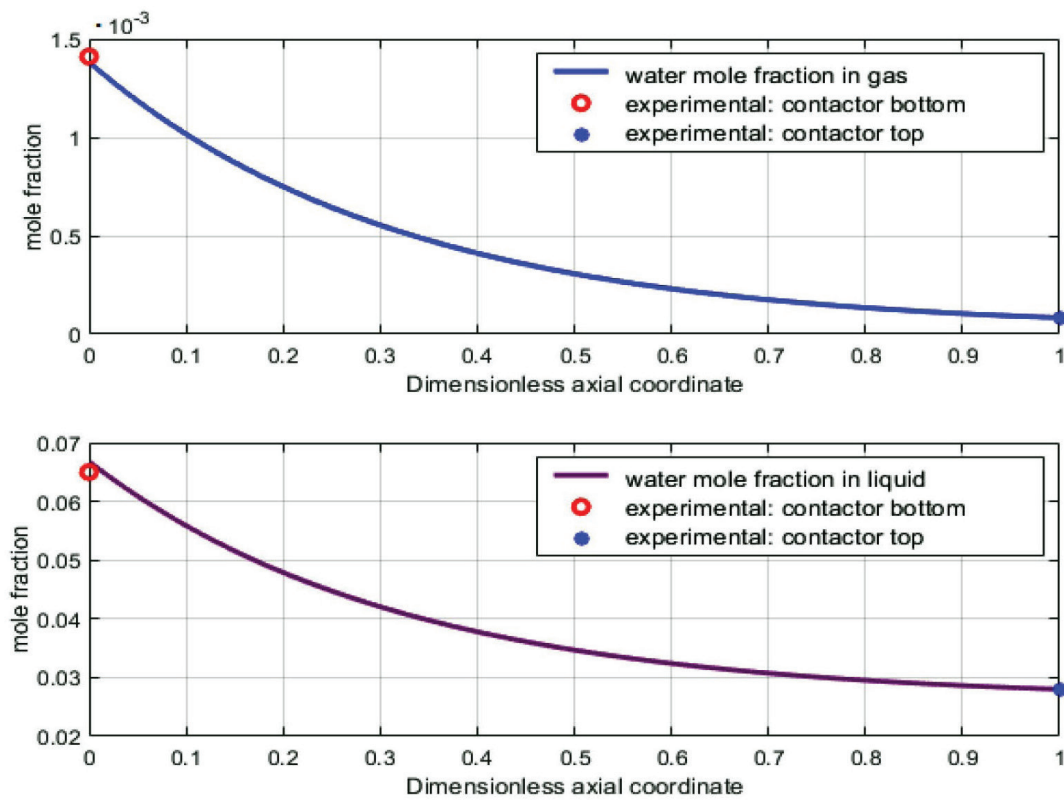


Fig. 7a – Example 2. Composition profiles (water mole fraction) of gas and liquid phases

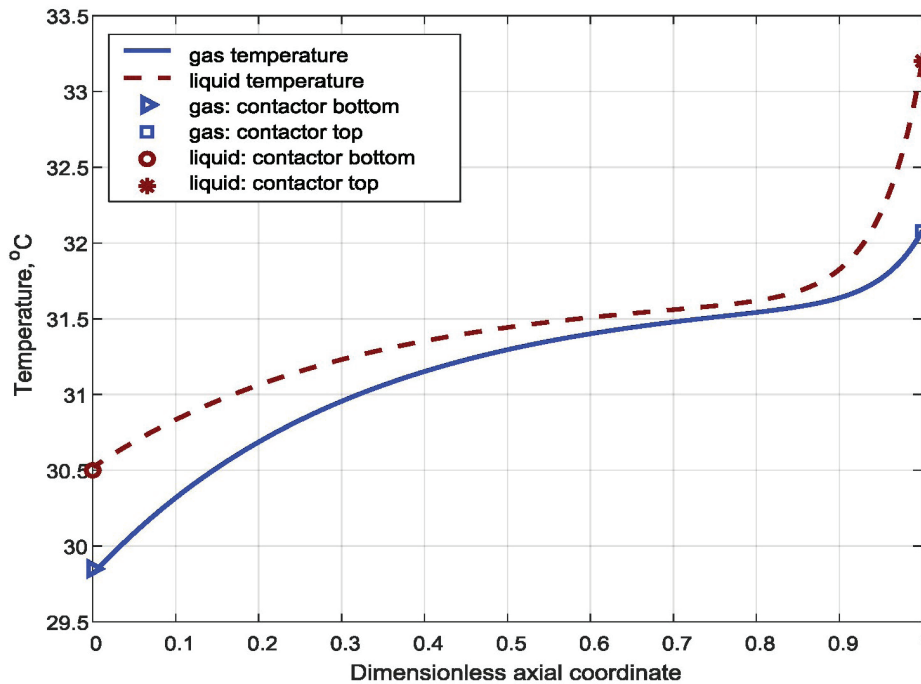


Fig. 7b – Example 2. Gas and liquid temperature profiles

The parameter values leading to the profiles in Figs. 6 and 7 are:

- Example 1: $K_y = 9.45 \text{ kmol m}^{-2} \text{ h}^{-1}$ and $\alpha_T = 315 \text{ W m}^{-2} \text{ °C}^{-1}$;
- Example 2: $K_y = 1.8 \text{ kmol m}^{-2} \text{ h}^{-1}$ and $\alpha_T = 55 \text{ W m}^{-2} \text{ °C}^{-1}$.

In both cases, tuned α_T values were relatively different than those predicted by correlation (5): 302 and 60 $\text{W m}^{-2} \text{ °C}^{-1}$, respectively. Because in all cases the differences are within the limit of $\pm 12\%$, no modification was made for the dependence of the Nusselt number on the Reynolds gas, the Reynolds liquid, and the Prandtl numbers.

For the correlation of the overall gas side mass transfer coefficient, a similar expression with that for the volumetric gas side mass transfer coefficient was used¹⁷:

$$K_y = \phi_1 (F_f)^{\phi_2} \cdot \left(\frac{\text{Re}_L}{h_L} \right)^{\phi_3} \cdot \text{Sc}_L^{0.33} \quad (19)$$

where:

$$h_L = \phi_4 \cdot \left(\frac{\eta_L \cdot w_L \cdot a_p^2}{\rho_L} \right)^{0.33} \quad (20)$$

$$\text{Re}_L = \frac{d_{SP} \cdot w_L \cdot \rho_L}{\eta_L \cdot \cos(\gamma)} \quad (21)$$

$$\text{Sc}_L = \frac{\eta_L}{\rho_L \cdot D_L} \quad (22)$$

The first three parameters, coefficient ϕ_1 , power of gas phase F factor, and the power of the liquid Reynolds number were evaluated in MATLAB® en-

vironment on the basis of collected plant data. The value of ϕ_4 was maintained the same as in our previous work¹⁷. The physical properties of the gas and the liquid phases were taken from the simulation cases build up for the validation/reconciliation of the process data. A comparison between the calculated values of K_y based on plant data and those predicted by Equation 19 for the estimated values of parameters ϕ_1 , ϕ_2 and ϕ_3 (0.058, 1, and 0.25, respectively) is shown in Fig. 8.

On the basis of the mass–heat transfer analogy²², the values of the overall gas side heat transfer coefficient can be calculated using the K_y values. A comparison between the predictions of Chilton–Colburn analogy and this work (Equation 5) is shown in Fig. 9.

In this specific case, the differences observed between the values predicted by the two methods show that the analogy underpredicts the value of the heat transfer coefficient. This is not only because Chilton–Colburn analogy characterizes just the conventional transfer phenomenon, not accounting for heat transfer fraction due to condensation²³, but also the contribution of the dried part and the effect of the packing conduction on heat transfer, to the effect of hydrocarbons absorption in TEG (not included in the mass balance), etc.

Stripping column

One of the most widely spread methods to increase the TEG purity is to further remove water from the TEG, while leaving the reboiler in a so-

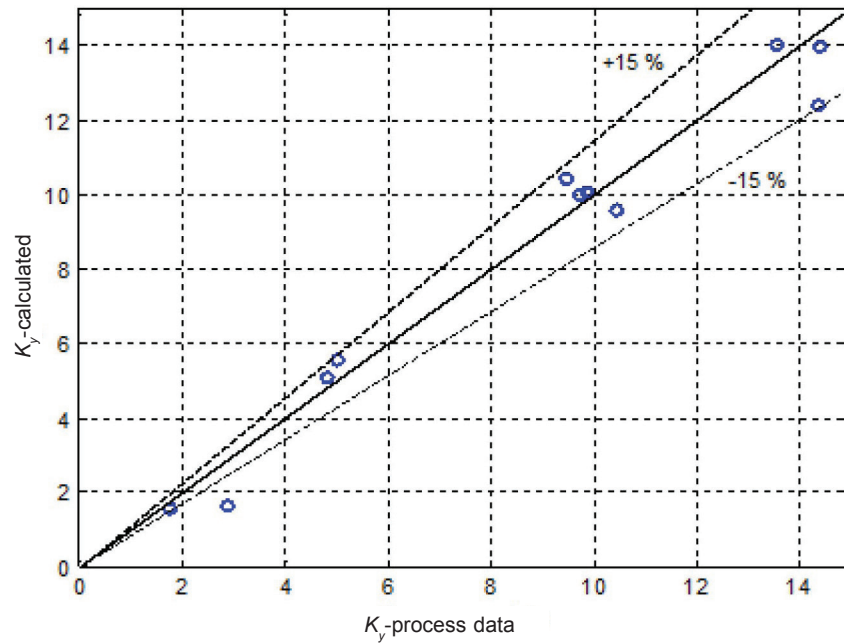


Fig. 8 – Comparison between calculated values of K_y (experimental data, $\text{kmol m}^{-2} \text{h}^{-1}$) and the values predicted by Equation 19 ($\phi_1 = 0.058$; $\phi_2 = 1$; $\phi_3 = 0.25$; $\phi_4 = 0.41$)

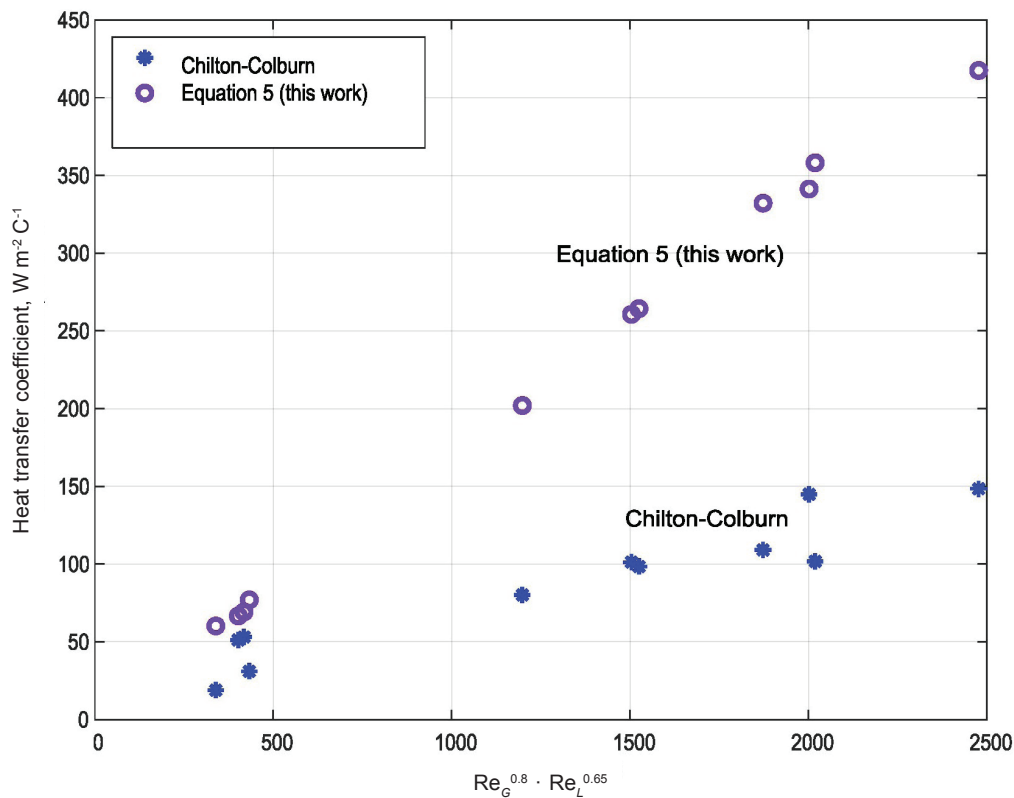


Fig. 9 – Heat transfer coefficient values: This work (Equation 5) versus Chilton – Colburn analogy

called “stripping column” (Fig. 2). The stripping gas is supplied through the surge drum, and from the top of the stripper is routed to the reboiler – still column block. The flow rate of the stripping gas is in direct connection with the desired TEG purity: increases from 98.8 (204 °C, no stripping gas) up to

99.8 w% (204 °C, around 25 N m^3 stripping gas per m^3 TEG solution) are possible²⁴.

The operating pressure in the regeneration unit is a key issue in the evaluation of the stripper number of theoretical stages necessary for achieving the targeted value of the TEG regeneration unit: at the

Table 2 – Typical stripping column operating parameters

Parameter	Value	Parameter	Value
Packing nominal specific surface	250 m ² m ⁻³	Operating pressure	1.05 bar
Temperature	202 °C	Packing height	2 m
Liquid load	33.5 m ³ m ⁻² h ⁻¹	Gas stripping density	160 N m ³ m ⁻² h ⁻¹
Water mole fraction in gas – gas inlet	0.0002	Water mole fraction in liquid – TEG inlet	0.0292
Water mole fraction in gas – gas outlet	0.6060	Water mole fraction in liquid – TEG outlet	0.0790

same temperature (200 °C) and the same stripping gas flow rate (7.5 N m³ m⁻³ TEG), the number of ideal stages is more than twice higher in the case of 1.25 bar, compared to 0.8 bar operating pressure. However, in most of the units, because of the possibility of oxygen (air) entering the towers with the consequence of increasing danger of explosion or fire, an operating pressure close to atmospheric pressure is chosen. It should also be noted that, in practice, because a total height over 2.5 m is not recommended for hydraulic reasons, the stripping gas flow rate is tuned to reach such height.

In order to evaluate the liquid-gas mass transfer flux, the process data covering liquid loads ranging from 20 to 40 m³ m⁻² h⁻¹ and F -factors ranging from 0.02 to 0.15 Pa^{0.5}, in 7 cases were collected and analyzed. According to Tsai¹⁸, the range of the liquid load indicates, for wetted to nominal packing area ratio for M250Y, a value close to 1. However, viewing the low values of the F -factor and the high operating temperature, in the case of the stripper, the mass transfer flux will be expressed on a volumetric basis. Because in all cases the temperature profile in the column was found close to isothermal temperature, a plug flow model describing gas and liquid phases composition along axial coordinate was used:

$$\frac{dL}{dz} = K_y a \cdot H \cdot S \cdot (y_w^* - y_w) \quad (23)$$

$$\frac{dG}{dz} = K_y a \cdot H \cdot S \cdot (y_w^* - y_w) \quad (24)$$

$$\frac{dy_w}{dz} = \frac{K_y a \cdot H \cdot S}{G} \cdot (y_w^* - y_w) - \frac{y_w}{G} \cdot \frac{dG}{dz} \quad (25)$$

$$\frac{dx_w}{dz} = \frac{K_y a \cdot H \cdot S}{L} \cdot (y_w^* - y_w) - \frac{x_w}{L} \cdot \frac{dL}{dz} \quad (26)$$

Boundary conditions:

$$\begin{aligned} \text{at } z = 0 \quad y_w &= y_w^{btm} & G &= G^{btm} \\ \text{at } z = 1 \quad x_w &= x_w^{top} & L &= L^{top} \end{aligned} \quad (27)$$

Calculated based on Equations 13 to 17, the water activity coefficient values at stripping column conditions (temperatures around 200–204 °C, pres-

sure close to atmospheric) is close to 1. Because such values are not confirmed by the experimental values published in the literature²⁵, the water equilibrium mole fraction was evaluated by adding a correction factor to the value calculated based on the Parrish *et al.*²¹ activity coefficient:

$$y_w^* = \phi_{strip} \cdot x_w \cdot \gamma_w \cdot \frac{p_w^{sat}}{P} \quad (28)$$

In Equation 28, a value of around 0.7 for ϕ_{strip} was finally chosen for the calculation of y_w^* .

The volumetric mass transfer coefficient, $K_y a$, was calculated in MATLAB[®] environment based on the minimization of the square sum of the differences between model predictions (Equations 23–26) and plant data. A typical set of stripper operating parameters is presented in Table 2.

The water mole fraction profiles in gas and liquid phases from Fig. 10 resulted in a $K_y a$ value of 31.45 kmol m⁻³ h⁻¹.

While taking into account the limited range of the operating parameter values, in order to express the variation of the volumetric mass transfer coefficient with stripping gas and liquid stream characteristics, a quite simple dependence was chosen:

$$K_y a = \beta_1 \cdot F_f^{\beta_2} \cdot L_0^{\beta_3} \quad (29)$$

In Equation 30, F_f is the average value of the F factor in the column, while L_0 is the liquid load (based on the TEG inlet volumetric flow rate).

The values of coefficients β_1 , β_2 , and β_3 were estimated by the minimization of the square sum of the differences between the $K_y a$ values, estimated as aforementioned, and the predictions of Equation 29. The accuracy of the prediction is shown in Fig. 11.

Despite the limited range of the process data (liquid load, F factor, gas and liquid temperature, etc.), Equation 29 is useful for the practical cases when estimation of the stripping gas flow rate is necessary. In the case of the stripper, for hydraulic reasons, structured packings manufacturers usually recommend a packing height of around 2 meters, while the main parameter to reach the water dew point required for natural gas transportation remains the stripping gas flow rate.

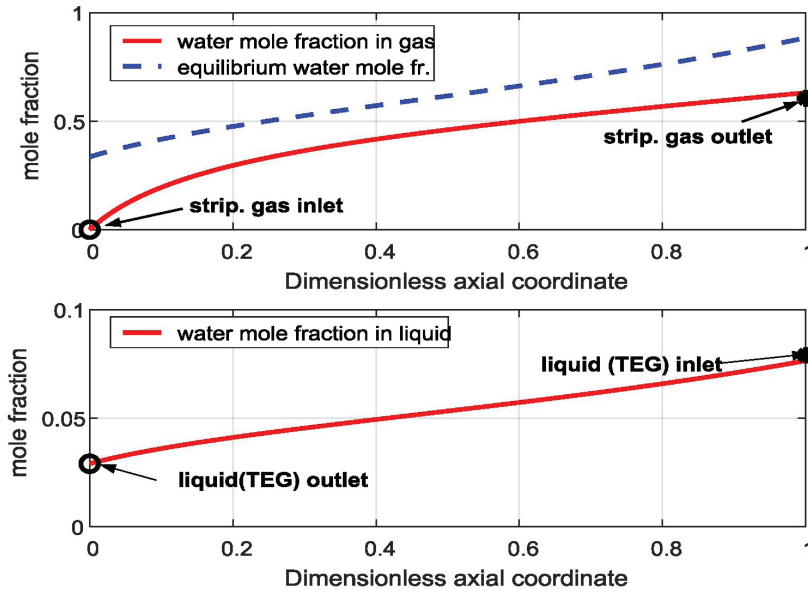


Fig. 10 – Water mole fraction profiles for the operating parameters from Table 2 ($K_y a = 31.45 \text{ kmol m}^{-3} \text{ h}^{-1}$)

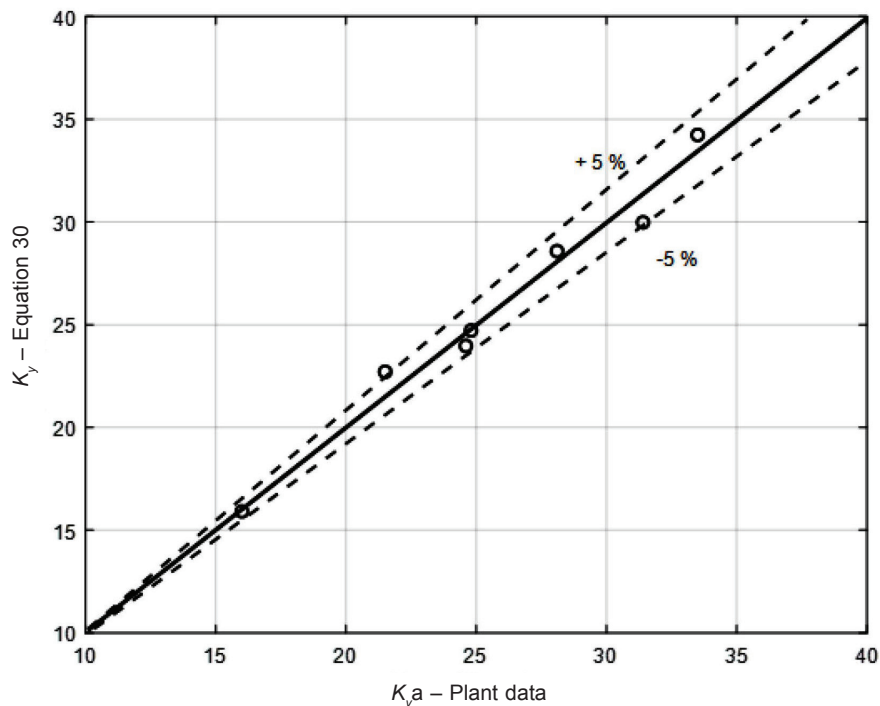


Fig. 11 – Stripping column: $K_y a$ values, $\text{kmol m}^{-3} \text{ h}^{-1}$, predicted by Equation 30 versus experimental data
Note: $\beta_1 = 30.1$; $\beta_2 = 0.407$; $\beta_3 = 0.26$

Conclusions

In this paper, the values of the overall gas phase mass transfer coefficients for absorption and stripping towers containing structured packings from natural gas TEG dehydration units were estimated by comparing plant data to the modeling simulation results by minimizing the square sum of the differences between models predictions and plant data.

On the heat transfer side, the direct contact heat transfer coefficient in the case of the absorption tower was estimated by analogy with the theory of multitubular heat exchangers, using process data validated through Aspen HYSYS.

In the case of the contactor, the correlations for gas side overall mass transfer and the direct contact heat transfer coefficients:

$$K_y = 0.058 \cdot (F_f)^1 \cdot \left(\frac{\text{Re}_L}{h_L} \right)^{0.25} \cdot \text{Sc}_L^{0.33} \quad (30)$$

$$\text{Nu}_G = 0.082 \cdot \text{Re}_G^{0.8} \cdot \text{Re}_L^{0.65} \text{Pr}_G^{1/3} \quad (31)$$

are based on industrial process data usually encountered in the gas dehydration units: pressures between 16 and 41 bar, gas velocities between 0.1 and 0.75 m s⁻¹, and liquid loads up to 2.5 m³ m⁻² h⁻¹. The heat flux, which also incorporates latent heat, was found to be around 2.5 times higher than the value calculated based on the Chilton – Colburn analogy.

In the case of the stripping column, in order to express the variation of the volumetric mass transfer coefficient with stripping gas and liquid stream characteristics, a quite simple dependence was finally validated:

$$K_y a = 30.1 \cdot F_f^{0.407} \cdot L_0^{0.26} \quad (32)$$

Such simple correlation is justified by the specificity of the process and by the limited range of the process data (liquid loads ranging from 20 to 40 m³ m⁻² h⁻¹ and *F*-factors ranging from 0.02 to 0.15 Pa^{0.5}).

Nomenclature

<i>a</i>	– effective interfacial area of the packing, m ² m ⁻³
<i>a_p</i>	– nominal interfacial area of the packing, m ² m ⁻³
<i>c_M</i>	– molar heat capacity, kJ kmol ⁻¹ °C ⁻¹
<i>c_{SL}</i>	– mass heat capacity of the liquid, kJ kg ⁻¹ °C ⁻¹
<i>D_L</i>	– water diffusion coefficient in liquid, m ² s ⁻¹
<i>d_{SP}</i>	– structured packing equivalent diameter, 4·ε _p /a _p , m
<i>F_f</i>	– <i>F</i> factor, Pa ^{0.5}
<i>g</i>	– gravitational constant, m s ⁻²
<i>G</i>	– gas molar flow rate, kmol h ⁻¹
<i>G₀</i>	– gas molar flow rate per square meter of transversal area, kmol m ⁻² h ⁻¹
<i>H</i>	– tower height, m
<i>h_L</i>	– liquid hold up, m ³ m ⁻³
<i>K_y</i>	– overall gas side mass transfer coefficient, kmol m ⁻² h ⁻¹
<i>K_ya</i>	– volumetric overall gas side mass transfer coefficient, kmol m ⁻³ h ⁻¹
<i>L</i>	– liquid molar flow rate, kmol h ⁻¹
<i>L_p</i>	– wetted perimeter in cross-sectional slice of packing, m
<i>L₀</i>	– molar liquid flow rate divided by column transversal area, kmol m ⁻² h ⁻¹
<i>L_M</i>	– liquid mass flow rate, kg h ⁻¹
<i>M</i>	– molecular weight, kg kmol ⁻¹

<i>Nu</i>	– Nusselt number
<i>P</i>	– pressure, bar
<i>Pr</i>	– Prandtl number
<i>P_w^{sat}</i>	– saturated water vapor pressure, bar
<i>Q_T</i>	– heat flux, kW
<i>Re</i>	– Reynolds number
<i>S</i>	– tower transversal area, m ²
<i>Sc</i>	– Schmidt number
<i>T</i>	– temperature, °C
<i>T_K</i>	– temperature, K
<i>w_G</i>	– gas velocity, m s ⁻¹
<i>w_L</i>	– liquid superficial velocity, m s ⁻¹
<i>x</i>	– mole fraction in liquid phase
<i>y_w</i>	– water mole fraction in the gas phase
<i>z</i>	– dimensionless axial coordinate
<i>γ</i>	– activity coefficient
<i>α_T</i>	– heat transfer coefficient, W m ⁻² °C ⁻¹
<i>ΔH_{abs}</i>	– water molar heat of absorption, kJ kmol ⁻¹
<i>ΔT_{ML}</i>	– mean logarithmic difference temperature, °C
<i>ε_p</i>	– bed voidage
<i>η_L</i>	– liquid viscosity, Pa·s
<i>ρ</i>	– density, kg m ⁻³
<i>σ</i>	– surface tension, N m ⁻¹
<i>Φ_w</i>	– water fugacity coefficient

Subscripts

<i>G</i>	– gas
<i>L</i>	– liquid
<i>ML</i>	– log –mean
<i>TEG</i>	– triethylene glycol
<i>w</i>	– water

Superscripts

<i>btm</i>	– bottom of column
<i>sat</i>	– saturation
<i>top</i>	– top of column
<i>*</i>	– equilibrium

Abbreviations

<i>DP</i>	– dew point
<i>EOS</i>	– equation of state
<i>HETP</i>	– height equivalent to a theoretical plate
<i>GPSA</i>	– GPSA Engineering Data Book
<i>PR</i>	– Peng-Robinson
<i>TEG</i>	– triethylene glycol

References

1. Kohl, A., Nielsen, R., Gas purification, Gulf Publishing, Houston Texas, 1997, pp. 946–1021.
2. Mokhatab, S., Poe, W., Speight, J., Handbook of natural gas transmission and processing, Gulf Professional Publishing, Waltham (MA), 2006, pp. 323 – 364.
doi: <https://doi.org/10.1016/B978-075067776-9/50014-2>
3. Netusil, M., Dittl, P., Comparison of three methods for natural gas dehydration, *J. Nat. Gas Chem.* **20** (2011) 471.
doi: [https://doi.org/10.1016/S1003-9953\(10\)60218-6](https://doi.org/10.1016/S1003-9953(10)60218-6)
4. Kong, Z. Y., Mahmoud, A., Liu, S., Sunarso, J., Revamping existing glycol technologies in natural gas dehydration to improve the purity and absorption efficiency: Available methods and recent developments, *J. Nat. Gas Sci. Eng.* **56** (2018) 486.
doi: <https://doi.org/10.1016/j.jngse.2018.06.008>
5. Salman, M., Zhang, L., Chen, J., A computational simulation study for techno-economic comparison of conventional and stripping gas methods for natural gas dehydration, *Chin. J. Chem. Eng.* **28** (2020) 2285.
doi: <https://doi.org/10.1016/j.cjche.2020.03.013>
6. Larachi, F., Lévesque, S., Grandjean, B. P. A., Seamless mass transfer correlations for packed beds bridging random and structured packings, *Ind. Eng. Chem. Res.* **47** (2008) 3274.
doi: <https://doi.org/10.1021/ie070718o>
7. Billet, R., Schultes, M., Prediction of mass transfer columns with dumped and arranged packings: Updated summary of the calculation method of Billet and Schultes, *Chem. Eng. Res. Des.* **77** (1999) 498.
doi: <https://doi.org/10.1205/026387699526520>
8. Hanley, B., Chau-Chyun, C., New mass-transfer correlations for packed towers, *AIChE J.* **58** (2012) 132.
doi: <https://doi.org/10.1002/aic.12574>
9. Tsai, R., Seibert, F., Eldridge, B., Rochelle, G., A dimensionless model for predicting the mass-transfer area of structured packing, *AIChE J.* **57** (2011) 1173.
doi: <https://doi.org/10.1002/aic.12345>
10. Flagiolo, D., Natale, F., Di Lancia, A., Erto, A., Characterization of mass transfer coefficients and pressure drops for packed towers with Mellapak 250.X, *Chem. Eng. Res. Des.* **161** (2020) 340.
doi: <https://doi.org/10.1016/j.cherd.2020.06.031>
11. Aspen HYSYS® V8.6 (2014), Aspen Tech simulation package (www.aspentech.com)
12. Twu, C. H., Tasone, V., Sim, W. D., Watanasiri, S., Advanced equation of state method for modeling TEG–water for glycol gas dehydration, *Fluid Phase Equilib.* **228** (2005) 213.
doi: <https://doi.org/10.1016/j.fluid.2004.09.031>
13. Watanasiri, S., Sachdev, R., Chang, Y.-T., Dymont, J., Dehydration with Aspen HYSYS: Validation of the CPA package, www.aspentech.com, AspenTech white paper, 2018.
14. Bahadori, A., New numerical model for solubility of light alkanes in triethylene glycol, *Korean J. Chem. Eng.* **24** (2007) 418.
15. Jou, F.-Y., Deshmukh, R. D., Otto, F. D., Mather, A. E., Vapor-liquid equilibria for acid gases and lower alkanes in triethylene glycol, *Fluid Phase Equilib.* **36** (1987) 121.
doi: [https://doi.org/10.1016/0378-3812\(87\)85018-5](https://doi.org/10.1016/0378-3812(87)85018-5)
16. GPSA Engineering Data Book, Gas Processors and Suppliers Association, Tulsa, OK, 12th edition, 2004, pp. 20.24 – 20.36.
17. Todinca, T., Filep, A. D., Muresan, T., TEG dehydration of natural gas: volumetric mass and heat transfer coefficients in packed bed absorbers, *Bull. Rom. Chem. Eng. Soc.* **1** (2014) 2.
18. Tsai, R. E., Mass transfer area of structured packings. PhD Thesis, University of Texas at Austin, (2010).
19. Spiegel, L., Bomio, P., A new method to design direct heat transfer sections in packed columns, in Darton, R., Distillation and Absorption '97, IChemE Rugby, 1997, pp. 991–998.
20. Saimpert, M., Puxty, G., Qureshy, S., Wardhaugh, L., Cousins, A., A new rate based absorber and desorber modelling tool, *Chem. Eng. Sci.* **96** (2013) 10.
doi: <https://doi.org/10.1016/j.ces.2013.03.013>
21. Parrish, W. R., Won, K. W., Baltatu, M. E., Phase behavior of the triethylene-glycol–water system and dehydration/regeneration design for extremely low dew point requirements, in Proc. Annu. Conv. Gas Process Assoc., San Antonio, TX, 1986, pp.202–210.
22. Fair, J. R., Bravo, J. L., Energy recovery by direct contact gas-liquid heat exchange, Proceedings from 10th Annual Ind. Energy Conference, Houston, TX, Sept., 13-15, 1988, pp. 264–269.
23. Enayatollahi, R., Nates, R. J., Anderson, T., The analogy between heat and mass transfer in low temperature cross-flow evaporation, *Int. Commun. Heat Mass Transf.* **86** (2017) 126.
doi: <https://doi.org/10.1016/j.icheatmasstransfer.2017.06.002>
24. Campbell, J. M., TEG Dehydration: Stripping Gas Charts for Lean TEG Regeneration, 2013, URL: <http://www.jmcampbell.com/tip-of-the-month/2013/07/teg-dehydration-stripping-gas-correlations-for-lean-teg-regeneration/> (28.10.2020).
25. GPA Editorial Review Board, Recent developments in gas dehydration and hydrate inhibition, in: Proceedings of the Laurance Reid Conference, Norman, Oklahoma, 1994, pp. 1–14.